Ayşenur PAMUKÇU

IZMIR KATIP CELEBI UNIVERSITY

2021

IZMIR KATIP CELEBI UNIVERSITY

GRADUATE SCHOOL OF NATURAL AND APPLIED SCIENCES

PREPARATION OF NOVEL SCAFFOLD SYSTEMS REINFORCED WITH MESOPOROUS SILICA NANOPARTICLES FOR BMP-2 DELIVERY AND IN VITRO INVESTIGATIONS

M.Sc. THESIS

Ayşenur PAMUKÇU

Department of Biomedical Technologies

Thesis Advisor: Assist. Prof. Dr. Didem ŞEN KARAMAN

Thesis Co-Advisor: Assoc. Prof. Dr. Ozan KARAMAN

JANUARY 2021

IZMIR KATIP CELEBI UNIVERSITY

GRADUATE SCHOOL OF NATURAL AND APPLIED SCIENCES

PREPARATION OF NOVEL SCAFFOLD SYSTEMS REINFORCED WITH MESOPOROUS SILICA NANOPARTICLES FOR BMP-2 DELIVERY AND IN VITRO INVESTIGATIONS

M.Sc. THESIS

Ayşenur PAMUKÇU

(Y180204001)

ORCID: 0000-0002-7650-4147

Department of Biomedical Technologies

Thesis Advisor: Assist. Prof. Dr. Didem ŞEN KARAMAN

Thesis Co-Advisor: Assoc. Prof. Dr. Ozan KARAMAN

JANUARY 2021

İZMİR KATİP CELEBİ ÜNİVERSİTESİ

FEN BİLİMLERİ ENSTİTÜSÜ

BMP-2 İLETİMİNDE KULLANILMAK ÜZERE MEZOPOROÖZ SİLİKA NANOPARÇACIKLAR İLE GÜÇLENDİRİLMİŞ YENİLİKÇİ DOKU İSKELESİ SİSTEMLERİNİN HAZIRLANMASI VE *İN VİTRO* İNCELENMELERİ

YÜKSEK LİSANS TEZİ

Ayşenur PAMUKÇU

(Y180204001)

ORCID: 0000-0002-7650-4147

Biyomedikal Teknolojiler Ana Bilim Dalı

Tez Danışmanı: Dr. Öğr. Üyesi Didem ŞEN KARAMAN

Tez Eş-Danışmanı: Doç. Dr. Ozan KARAMAN

OCAK 2021

Ayşenur PAMUKÇU, a **M.Sc.** student of **IKCU Graduate School of Natural and Applied Sciences**, successfully defended the thesis entitled **"Preparation of Novel Scaffold Systems Reinforced with Mesoporous Silica Nanoparticles for BMP-2 Delivery and *In Vitro* Investigations**", which she prepared after fulfilling the requirements specified in the associated legislations, before the jury whose signatures are below.

Thesis Advisor :

Assist. Prof. Dr. Didem ŞEN KARAMAN .....
İzmir Kâtip Çelebi University

Thesis Co-Advisor :

Assoc. Prof. Dr. Ozan KARAMAN .....
İzmir Kâtip Çelebi University

Jury Members :

Assist. Prof. Dr. Ahmet AYKAÇ .....
İzmir Kâtip Çelebi University

Assoc. Prof. Dr. Nazlı SARIKAHYA .....
Ege University

Date of Defense : 29.01.2021

To my family

FOREWORD

I would like to express my sincere gratitude to my supervisor, Assist. Prof. Dr. Didem ŞEN KARAMAN for her support and guidance during my MSc study. I have been so lucky to have such supervisor who affects my academic career and personal life in a positive attitude with her enthusiasm, knowledge and determination.

I would also like to thank my co-supervisor Assoc. Prof. Dr. Ozan KARAMAN for his support and valuable comments during my studies.

I would like to acknowledge the members of Tissue Engineering and Regenerative Medicine Laboratory, and Bioanalytical and Biosensor Laboratory for their technical supports and comments on some experiments. I would also like to acknowledge Faculty of Medicine and Faculty of Pharmacy for their technical assistance.

I would also like to thank all members of NanoMED&BioMAT Lab, especially Nursu ERDOĞAN, for providing fun and a peaceful working environment during my studies.

The Scientific and Technological Research Council of Turkey (TUBITAK) are greatly acknowledged for financially supporting me under the program of "2210/C National MSc/MA Scholarship Program in the Priority Fields in Science and Technology" during my MSc study. I would like to thank Izmir Katip Celebi University, Coordination Office of Scientific Research Projects for supporting this thesis. I would also like to acknowledge Fidia Farmaceutici S.p.A. for kindly providing HYAFF®11 polymer.

I would like to thank my family for their patience and support during my education. I would also like to thank Nihal KARAKAŞ and Büşra KÖSE for their valuable friendship.

I would like to express my special thanks to my partner, Burak AKBUĞDAY, for his motivation, unlimited support and confidence in my skills.

January 2021

Ayşenur PAMUKÇU

TABLE OF CONTENTS

Page

LIST OF TABLES

Page

LIST OF FIGURES

Page

ABBREVIATIONS

ECM : Extracellular matrix

BMP : Bone morphogenetic protein

ALP : Alkaline phosphatase

PEG : Polyethylene glycol

PEGDMA : Polyethylene glycol dimethacrylate

PLAF : Poly(lactide fumarate

PLEOF : Poly(lactide-co-ethylene oxide fumarate)

MSN : Mesoporous silica nanoparticle

MCM41 : Mobil composition of matter No. 41

DEX : Dexamethasone

TBC : True bone ceramics

SiO_2 : Silicon dioxide

MC3T3-E1 : Mouse osteoblastic cell line

DFO : Deferoxamine

SEM : Scanning electron microscopy

DLS : Dynamic light scattering

L929 : Murine fibroblast cell line

DMF : Dimethylformamide

FMOC : 9-Fluorenylmethyloxycarbonyl

HBTU : (2-(1H-benzotriazol-1-yl)-1,1,3,3-tetramethyluronium hexafluorophosphate

DIEA : N,N-Diisopropylethylamine

TFA : Trifluoroacetic acid

TIPS : Triisopropylsilane

TEOS : Tetraethyl orthosilicate

CTAB : Cetyltrimethyl ammonium bromide

TEA : Triethanolamine

APTES : (3-aminopropyl)triethoxysilane

HEPES : 4-(2-Hydroxyethyl)piperazine-1-ethanesulfonic acid

BET : Brunauer-Emmett-Teller

STEM **:** Scanning transmission electron microscope

PB **:** Phosphate buffer

PBS **:** Phosphate-buffered saline

DMEM **:** Dulbecco’s Modified Eagle Medium

FBS **:** Fetal Bovine Serum

DMSO **:** Dimethyl sulfoxide

PDI **:** Polydispersity index

PREPARATION OF NOVEL SCAFFOLD SYSTEMS REINFORCED WITH MESOPOROUS SILICA NANOPARTICLES FOR BMP-2 DELIVERY AND *IN VITRO* INVESTIGATIONS

ABSTRACT

Multifunctional scaffolds capable of mimicking native extracellular matrix environment and presenting bioactive molecules are attractive for tissue engineering applications. Hydrogels are one of the promising classes of scaffolds of which the mechanical property and biological activity can be improved with the advancements in the biomaterial science. In this study, the impact of the different biomaterials on the physicochemical and biological properties of polyethylene glycol dimethacrylate (PEGDMA) hydrogels were investigated. During studies, the mechanical properties of the hydrogels were tuned with the integration of the mesoporous silica nanoparticles. Mesoporous silica nanoparticles to be incorporated into hydrogels were synthesized by water-oil biphase stratification approach and characterized by scanning electron microscopy, dynamic light scattering and nitrogen sorption analyses. Moreover, mesoporous silica nanoparticles were utilized as reservoirs for the delivery of BMP2-derived peptide as a bioactive molecule in hydrogel structure. To construct an environment similar to native tissues, hydrogels were mixed with the hyaluronic acid derivative. After the fabrication of PEGDMA composite hydrogels, mechanical properties were investigated by compression test and swelling studies. The *in vitro* cytocompatibility of multifunctional scaffolds were evaluated on L929 cell line by encapsulation of cells within the hydrogel matrix. Results showed that mesoporous silica nanoparticle and hyaluronic acid incorporation into PEGDMA hydrogels resulted in a slight decrease in swelling degree. On the other hand, *in vitro* viability assays demonstrated that functionalized hydrogels did not generate a cytotoxic effect against cells. In conclusion, this study proves that the utilization of mesoporous silica nanoparticles enables the fabrication of hydrogels with controllable mechanical and biological properties.

BMP-2 İLETİMİNDE KULLANILMAK ÜZERE MEZOPOROÖZ SİLİKA NANOPARÇACIKLAR İLE GÜÇLENDİRİLMİŞ YENİLİKÇİ DOKU İSKELESİ SİSTEMLERİNİN HAZIRLANMASI VE *İN VİTRO* İNCELENMELERİ

ÖZET

Doğal hücre dışı matris ortamını taklit edebilen ve biyoaktif maddeleri içeren çok işlevli doku iskelelerinin doku mühendisliği uygulamalarında kullanımı ilgi çekmektedir. Hidrojeller mekanik özellikleri ve biyolojik aktiviteleri biyomalzeme bilimindeki ilerlemeler sayesinde geliştirilebilen umut verici doku iskelesi sınıflarından birisidir. Bu çalışmada, farklı biyomalzemelerin polietilen glikol dimetilakrilat (PEGDMA) hidrojelinin fizikokimyasal ve biyolojik özelliklerine olan etkisi incelenmiştir. Çalışmalar sırasında, hidrojelin mekanik özellikleri yapısına mezoporöz silika nanoparçacıkların entegrasyonu ile modifiye edilmiştir. Hidrojel yapısına eklenen mezoporöz silika nanoparçacıkları iki fazlı tabakalaşma yaklaşımı ile sentezlenmiş ve taramalı electron mikroskobu, dinamik ışık saçılımı ve por boyut analizleri ile karakterize edilmiştir. Buna ek olarak, mezoporöz silika nanoparçacıkları hidrojel yapısında model biyoaktif molekül olarak kullanılmış olan BMP2 peptidinin taşınımı için kullanılmıştır. Doğal dokulara benzer bir ortam oluşturmak için hidrojeller ayrıca hyalüronik asit ile zenginleştirilmiştir. PEGDMA kompozit hidrojellerinin mekanik özellikleri basma testi ve su tutma kapasitesi analizi ile incelenmiştir. Çok işlevli doku iskelelerinin *in vitro* biyouyumluluğu L929 hücrelerinin hidrojel matrisi içinde enkapsülasyonu ile test edilmiştir. Sonuçlar mesoporöz silika nanoparçacıkların ve hyalüronik asidin PEGDMA hidrojeline entegrasyonunun su tutma kapasitesini az miktarda düşürdüğünü göstermiştir. Bunun yanı sıra, yapılan *in vitro* testler fonksiyonelleştirilmiş hidrojellerin hücrelere karşı sitotoksik bir etki oluşturmadığını göstermiştir. Sonuç olarak, bu çalışma mezoporöz silika nanoparçacıkların kullanımının mekanik ve biyolojik özellikleri kontrol edilebilir doku iskelelerinin üretimine olanak sağladığını göstermiştir.

1. INTRODUCTION

Bone is a dense connective tissue composed of bone cells and extracellular matrix (ECM) involving an organic phase and a mineral phase. The organic phase of ECM contains growth factors, proteoglycans, and cytokines as well as collagen type I which is the major component of the organic phase providing flexibility and elasticity to the bone. The mineral phase is formed by hydroxyapatite nanocrystals and confer strength and rigidity to the bone. Bone cells, on the other hand, include three principal cell types which are osteoblasts, osteocytes, and osteoclasts, crucial for bone formation (osteogenesis) and bone remodeling.

Bone remodeling is the replacement of injured bone tissue by new bone tissue which occurs with the aid of osteoclasts, osteoblasts, and osteocytes. During the first step of remodeling, osteoclastic resorption occurs, in other words, bone matrix and bone mineral is degraded enzymatically by osteoclast cells. Afterward, osteoblasts are recruited to the site of resorption and bone formation takes place by differentiation of those cells. This process is followed by matrix mineralization and osteocyte production. The bone remodeling process terminates when resorbed bone by osteoclasts is completely replaced [1,2].

From the molecular aspect, numerous growth factors account for the complex process of osteogenesis and bone remodeling [3,4]. Among them, bone morphogenetic proteins (BMPs) are the most promising growth factors capable of inducing new bone formation upon differentiation of bone marrow mesenchymal stem cells into osteoblast cells or promote the proliferation of osteoblasts and chondrocytes [5]. Studies have also shown that BMPs stimulate the healing of bone defects or fractures [6]. BMP family members show different degrees of osteoinductive activity of which BMP2, BMP9, and BMP7 show the strongest activity on osteogenesis. BMP2 is an acidic glycoprotein having 114 amino acid residues with a molecular weight of 32 kDa. BMP2 confers its osteoinductive activity on mesenchymal stem cells through binding type I/II serine-threonine kinase receptors on the target membrane, resulting in activation of Smads signaling pathway as shown in Figure 1.1. Activation of BMP2-mediated signal transduction pathway results in transcriptional regulation of genes

related to osteogenesis such as osteocalcin, alkaline phosphatase, type-I collagen and osterix [7,8].

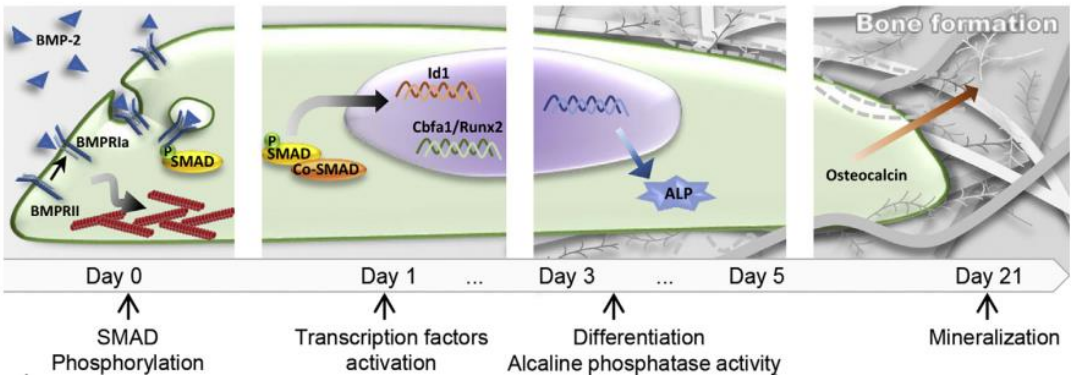

Figure 1.1 Demonstration of major steps of osteogenic differentiation upon induction by BMP2 protein. Figure is adapted from [9].

The three-dimensional bio-mimicked scaffolds have a tremendous role in tissue engineering applications such as in bone remodeling process. It is known that cells interact with the ECM, which is responsible for providing mechanical strength to cells, modulating cell behavior, and controlling the release of growth factors [10]. However, scaffolds comprising a single component cannot generally meet all the requirements for efficient tissue regeneration. An ideal scaffold matrix should possess bioactive molecules to cells and provide mechanical support while structurally mimicking the native ECM as shown in Figure 1.2. It is therefore important to functionalize scaffolds to be able to obtain a cellular response as observed in the native ECM environment.

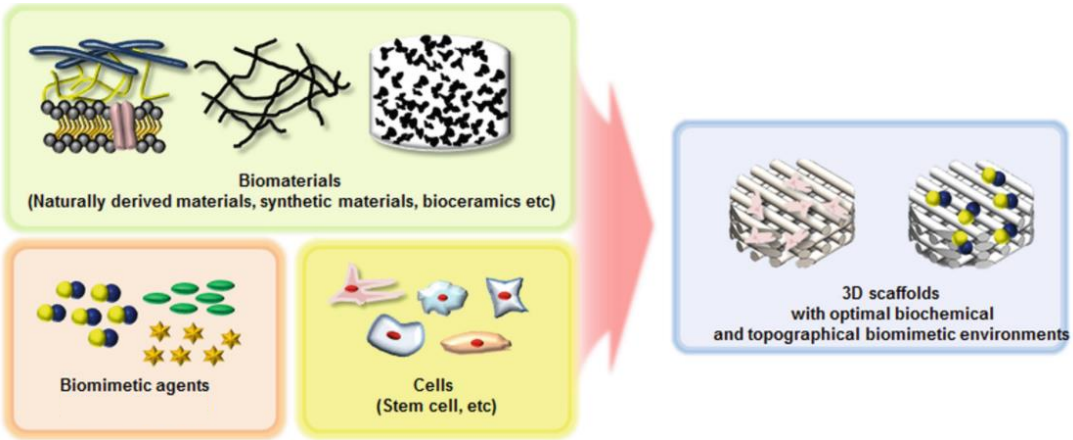

Figure 1.2 Components of an ideal scaffold for tissue engineering applications. Figure is adapted from [11].

Hydrogels are three-dimensional polymeric networks enabling exchange of nutrients and oxygen due to their permeable texture (Figure 1.3). Besides, they could protect cells from environmental factors such as mechanical stress and cytotoxic products. Hydrogel scaffolds can be fabricated by using a diverse range of polymers of natural or synthetic origin. Bioinert synthetic hydrogel scaffolds have attracted great interest and they can be fabricated using polyethylene glycol (PEG) and PEG-derivatives (PEG-diacrylate, PEG-methacrylate) upon crosslinking by free-radical photopolymerization methods. The physicochemical properties of PEGDMA hydrogels could be modulated by changing the polymer concentration for application of interest [12]. Nevertheless, PEG hydrogels exhibit low cell adhesion and proliferation which require further improvement. In general, hydrogel scaffolds fabricated by PEG and its derivatives should possess bioactive cues to show desired activity [13,14].

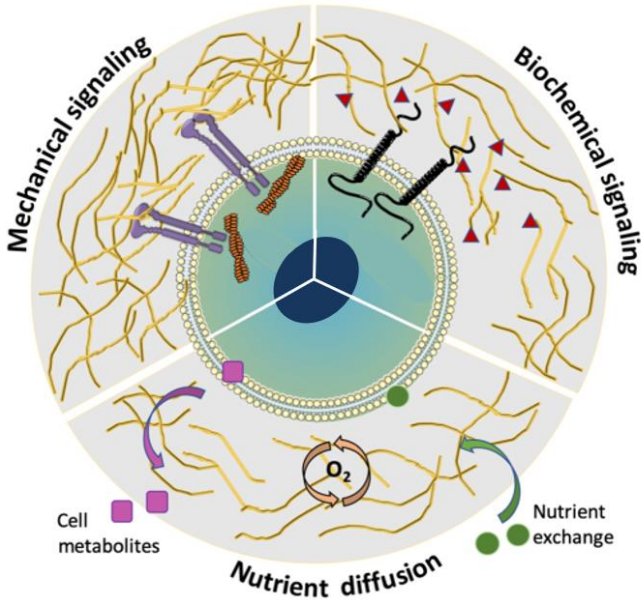

Figure 1.3 Benefits of hydrogels during development of three-dimensional bio-mimicked scaffolds. Figure is adapted from [15].

Hyaluronic acid is one of the important components of extracellular matrix and acts in regulation of cell migration, differentiation, and angiogenesis through binding CD44 cell surface receptors [16]. Hyaluronic acid also promotes osteogenesis of mesenchymal stem cells by binding to CD168 receptors. Hyaluronic acid shows good biocompatibility with cells when used as tissue engineering scaffolds due to its

hydrophilicity and non-toxic degradation products [17]. The presence of hydroxyl and carboxyl groups in the structure of hyaluronic acid enables porous hydrogel formation with the aid of chemical modification or crosslinking [18,19]. However, rapid absorption of hyaluronic acid impedes the stability of hydrogel scaffolds and therefore requires enhancement. One of the approaches is to chemically modify hyaluronic acid through esterification reactions to improve its stability and prolong its maintenance in aqueous environments. HYAFF®11, benzyl ester of hyaluronic acid, is a biopolymer synthesized by esterification of sodium hyaluronate with the benzyl alcohol for use in tissue engineering and drug delivery studies [20]. Mermerkaya et al. used HYAFF®11 in the form of fiber membranes to evaluate the osteoblastic activity of the membranes *in vivo.* Results showed that presence of hyaluronic acid-based biomaterial in bone defect sites increases bone healing [21]. Though, utilization of pure hyaluronic acid hydrogels, such as HYAFF®11, in bone tissue engineering is still precluded because of its weak mechanical properties in comparison to human bone. As an alternative method, hyaluronic acid could serve as a bioactive additive in synthetic scaffolds such as PEG [22].

Even though improvement of cell adhesion and proliferation properties of hydrogels could be achieved with the aid of bioactive polymers of high molecular weight, enhancement of hydrogel properties by small bioactive molecules is hindered due to high diffusion kinetics. Researchers have also encountered this problem during the utilization of BMP2 protein and peptides derived from it. Although the osteoinductive activity of the BMP2 growth factor has paved the way for the use of BMP2 in bone tissue engineering, it generally diffuses out of the target site upon administration and result in undesired biological effects on surrounding tissues as tumorigenesis, heterotopic ossification, and bone overgrowth [7]. The diffusion from the target site also requires the use of high doses of BMP2 to acquire bone formation. In addition to such safety concerns, utilization of growth factors in therapeutic applications has been questioned because of their high-cost production. Such a cost-effective approach is to use peptide sequences of BMP2 growth factor of which capable of mimicking the bioactivity. The knuckle epitope of BMP2, having the sequence of KIPKASSVPTELSAISTLY, has been investigated for its osteogenic activity and showed promising results [23,24]. For delivery of such short mimicking peptides

various approaches have been used to provide sustained and controlled release of bioactive molecules for modulating the stem cell fate. Recent advances in biomaterials science and nanotechnology have held a great promise in tissue engineering and led to significant progress for the development of scaffolds with multifunctionality [25]. To meet the requirement of an ideal tissue engineering scaffold, nanoparticle embedded scaffold matrices with modified biodegradability, biomechanical strength, bioactive properties, and defined three-dimensional structure could be fabricated [26,27].

Madl et al. (2014) incorporated BMP2 mimicking peptides into two- and three-dimensional alginate hydrogels for investigating the capacity of BMP2 mimicking peptide on osteogenesis and the effect of different culture environments [23]. BMP2 mimicking peptide was physically adsorbed on two-dimensional alginate surfaces while maleimide-thiol chemistry was used for peptide conjugation onto three-dimensional alginate scaffolds. Results showed that ALP activity and Smad signaling induction of the cells in three-dimensional culture was higher in comparison to the two-dimensional culture environment. However, the possibility of cross-reactions with the lysine residues in the BMP2 mimicking peptide has prevented the use of carbodiimide chemistry for the conjugation of the peptide to alginate hydrogel. This shows the sensitivity of the BMP2 mimicking peptide to covalent coupling strategies which may even lead to low efficiency or activity loss. Chen et al. (2017) employed the similar strategy for immobilization of BMP2 mimicking peptide on a composite scaffold consisted of chitosan and hydroxyapatite [28]. In their study, *in vivo* ectopic bone formation revealing osteoinductive activity and repair in cranial bone defect model showing bone regeneration were observed in groups containing BMP2 peptide with the aid of hydroxyapatite which constitutes the mineral phase of bone tissue. A comprehensive study investigating the effect of different matrix stiffnesses along with different biomolecules on stem cell fate was carried out by Zouani et al. (2013) with a two-dimensional culture system [27]. They showed that osteogenic differentiation of human mesenchymal stem cells was acquired at the stiffness of 45-49 kPa with poly(acrylamide-co-acrylic acid) being the hydrogel matrix under study. The presence of BMP2 mimetic peptide on the surface of the stiff hydrogel matrix resulted in osteogenic differentiation as expected. Interestingly, the presentation of BMP2 mimicking peptide on soft hydrogel matrix, where normally myogenic differentiation

occurs with the proper adhesion molecule, ended up with osteogenic differentiation. Even though the cooperation between ECM components and growth factors play a critical role in osteogenic differentiation, the capacity of biochemical molecules to inhibit ECM stiffness was of importance.

The other, yet promising, approach is to use nanoparticles for the immobilization of BMP2-derived peptide to increase residence time along with the decrease in the diffusion. As is stated above, it is generally necessary to retain the release of the growth factors at a specific threshold and for a certain time interval to induce regeneration at the target site. The utilization of nanoparticles, therefore, can be advantageous for the controlled and sustained delivery of bioactive molecules. The incorporation of nanoparticles into scaffold matrix results in improved cell adhesion and proliferation. Mohammadi et al. (2018) developed a scaffold system in which hydroxyapatite nanoparticles were used for enhancing cell attachment and liposomal nanoparticles for encapsulation and controlled release of BMP2 peptide [29]. BMP2 peptide was released in a sustained manner from the liposomal nanoparticles covalently attached to the scaffolds. In the study, a higher level of ALP and improved ectopic bone formation was attributed to the sustained release pattern of BMP2 peptide. Synthetic polymeric nanoparticles were also utilized for the grafting of BMP2 peptide to be used in osteogenic differentiation studies. Mercado et al. (2014) utilized poly(lactide fumarate) (PLAF) and poly(lactide-co-ethylene oxide fumarate) (PLEOF) polymer to produce self-assembled nanoparticles to which BMP2 peptide or protein grafted. Results demonstrated that grafting of either BMP2 peptide or protein to PLAF-PLEOF nanoparticle significantly enhanced osteogenic expression in comparison to their free forms [30]. BMP2 peptide-grafted PLAF nanoparticles were also utilized in a study to investigate the differentiation capability of mesenchymal stem cells and results demonstrated that BMP2 grafted nanoparticles exhibited greater affinity to cell surface receptors of BMP, resulting in stronger signal pathway activation [31]. Apart from polymeric nanoparticles, inorganic nanoparticles have also shown potential for BMP2 peptide delivery. Gold nanoparticles decorated with hyaluronic acid have been used for covalent conjugation of BMP2 peptide, followed by improved intracellular uptake of the peptide and increased gene expression for osteogenesis [32].

Mesoporous silica nanoparticles (MSNs) are potential candidates for use in biomolecule delivery systems and in combination with scaffolds for tissue engineering applications as summarized in Figure 1.4 [33]. Biocompatibility, biodegradability, low cytotoxicity, ease functionalization, and high specific surface area of MSNs have attracted attention for tissue engineering applications. The utilization of MSNs for stem cell tracking and the ability to guide the proliferation and adhesion of stem cells has already been investigated [34–36]. The high surface-area-to-volume ratio and mesoporous structure of MSNs enable the loading and sustained release of various molecules in high amounts. Besides, textural properties of MSNs such as pore size and pore volume can easily be manipulated by synthesis chemistry as pore structure is a determining factor for loading capacity and release rate [37,38]. Convenient modification of MSNs also enables a surface bearing different functional groups, which provides the opportunity to conjugate or load a variety of bioactive molecules. Zhou et al. (2015) covalently grafted BMP2 peptide on the surface of amine-modified MCM41 type MSNs following loading of dexamethasone into the pores of MSNs [38]. Results showed that DEX@MSN-pep enhanced ALP activity, calcium deposition, and expression of RUNX2 protein responsible for BMP2 pathway activation. However, the authors used 2-3 nm pore sized-MCM41 type MSNs which is inappropriate for effective BMP2 peptide loading because of its size.

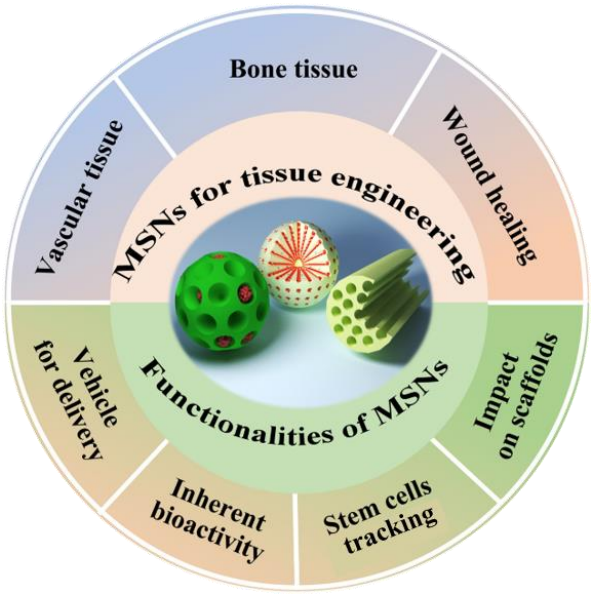

Figure 1.4 Schematic representation of functionalities and application areas of mesoporous silica nanoparticles in tissue engineering. Figure is adapted from [39].

MSNs have recently been used in combination with three-dimensional scaffold systems for the delivery of BMP2 peptide. One of these scaffold systems was developed by Cui et al. (2018) where hollow MSNs with enlarged pores were used for controlled release of BMP2-related peptide, P28 (S[PO_4]DDDDDDDKIPKASSVPTELSAISTLYL), from true bone ceramics (TBC) scaffold [40]. In the study, hollow MSNs with enlarged pores were synthesized by coating solid SiO_2 core with mesoporous SiO_2 shell, while using decane as a pore expander in the shell formulation. Results showed that hollow MSNs retarded the release of P28 in the TBC scaffold and promoted osteogenic differentiation of MC3T3-E1 cells. The developed system also induced bone regeneration *in vivo* in a critical size bone defect model in 6 weeks. Yao et al. (2018) developed a dual drug-delivery system for the delivery of BMP2 peptide and deferoxamine (DFO). In the study, BMP2 protein was loaded into pore-expanded MSNs and DFO was conjugated with chitosan for incorporation into three-dimensional gelatin scaffolds. Henceforth, different release rates were obtained while maintaining osteogenic and angiogenic activity [41]. These studies show the potential of MSNs to have an important role in tissue engineering applications.

In the light of literature findings, the objective of this thesis is to develop a multifunctional scaffold system capable of mimicking the native ECM tissue for the growth and differentiation of mesenchymal stem cells. The scaffold design encompasses components capable of *i)* providing a three-dimensional environment for cells as in natural tissues, *ii)* supporting the main scaffold with a natural polymer to mimic the native ECM tissue, *iii)* providing growth factors via nanoparticles to promote differentiation (Figure 1.5).

During studies, the three-dimensional environment was generated with polyethylene glycol dimethyl acrylate (PEGDMA) polymer by employing photo-polymerization approaches. PEGDMA and other PEG derivatives have been extensively used as hydrogels in tissue engineering applications since they are inert, biocompatible, hydrophilic, and easy to modulate [12,42,43]. The three-dimensional environment created with PEGDMA hydrogel was improved by the addition of a hyaluronic acid derivative, HYAFF®11 polymer. HYAFF®11 is a benzyl ester of hyaluronic acid which is biocompatible and biodegradable and used in drug delivery, tissue repair, and

regeneration studies. Hyaluronic acid is known to bind several cell surface receptors and favors bone deposition [44]. Hence, the presence of HYAFF®11 is expected to increase the biocompatibility of PEGDMA hydrogel while mimicking natural tissue. In addition to this, MSNs were incorporated into the HYAFF®11-PEGDMA (H-PEGDMA) hydrogel as the vehicle for the delivery of BMP2-derived peptide in order to constitute an environment capable of triggering osteogenic differentiation. To achieve a high loading amount of BMP2-derived peptide, a new sol-gel approach based on water-oil biphase stratification was employed to synthesize MSNs. The biphase stratification approach enables the synthesis of MSNs with larger pores, i.e., 10 nm and above, which is beneficial for reserving the large cargo biomolecules [45]. Characterization of MSNs was investigated by scanning electron microscopy (SEM), dynamic light scattering (DLS), zeta potential, and nitrogen sorption analyses. BMP2-derived peptide synthesized by solid-phase peptide synthesis method was then loaded into pores of MSNs due to electrostatic interactions. After incorporation of MSNs at different amounts and HYAFF®11 into PEGDMA hydrogel structure, changes in physical properties of the final form of the scaffold were investigated with compression and swelling tests. Biocompatibility of the MSN/H-PEGDMA hydrogels was evaluated on the L929 cell line in the last step by encapsulating the cells with MSN/H-PEGDMA hydrogels. Thus, the capability of the developed scaffold design for three-dimensional tissue engineering applications was also investigated.

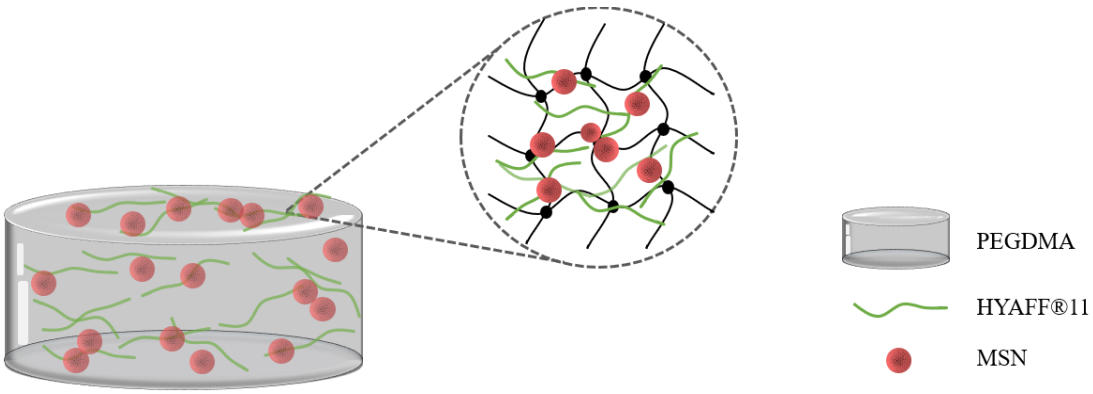

Figure 1.5 Basic demonstration of the multifunctional scaffold system developed with PEGDMA, HYAFF®11 and MSNs.

2. EXPERIMENTS

2.1 BMP2-derived Peptide Synthesis

BMP2-derived peptide, KIPKASSVPTELSAISTLY, synthesis was performed using aapptec Focus Xi peptide synthesizer. For reaction, 400 mg of resins was loaded into the reaction vessel of the peptide synthesizer. Resins were first incubated in dimethylformamide (DMF) solvent for 30 min to achieve swelling. Swelled resins were then treated with deprotection solution for 9-Fluorenylmethyloxycarbonyl (Fmoc) groups to be removed. Amino acid solutions corresponding to a 5-fold molar excess of the resin prepared in DMF were used for coupling. During synthesis, 20% (v/v) of cyclohexylamine in DMF was used for Fmoc deprotection while 0.32 M (2-(1H-benzotriazol-1-yl)-1,1,3,3-tetramethyluronium hexafluorophosphate (HBTU) and 0.2 M N,N-Diisopropylethylamine (DIEA) were used for amino acid coupling.

After coupling of all amino acids, cleavage of the peptides from the resins was carried out by incubating resins in a solution comprising 95% trifluoroacetic acid (TFA), 2.5% triisopropylsilane (TIPS), and 2.5% H_2O for 2h. The free peptides in the solution were then collected by eluting into cold diethyl ether and centrifugation at 4500 rpm for 15 mins. The supernatant was discarded, and peptide powder was kept at the fume hood overnight to evaporate excess diethyl ether. On the following day, the peptide powder was dissolved in dH_2O and stored at -80^oC. Peptide products were then obtained by lyophilization and stored at -20^oC for further use.

2.2 Mesoporous Silica Nanoparticle (MSN) Synthesis and Characterization

2.2.1 MSN synthesis

Synthesis of MSNs was performed based on the protocol by Shen et al. (2014) with minor modifications [46]. MSNs having 20% tetraethyl orthosilicate (TEOS) (v/v) were chosen for the experiments and a 200 ml batch was synthesized. For the synthesis, TEOS was used as the silica source and cetyl-trimethyl-ammonium-bromide (CTAB) as a structure-directing agent. For the basic aqueous phase, 17 g of CTAB was carefully added into 150 ml of distilled H_2O. After CTAB completely dissolved, 400

µl of triethanolamine (TEA) was pipetted into the solution. The resulting mixture was stirred at 60°C and 150 rpm for 1h. Thereafter, the upper oil phase was prepared by homogeneously mixing 10 ml TEOS in 40 ml cyclohexane solution. The upper oil phase was then gently pipetted onto the aqueous phase. The synthesis solution was kept at 60°C for 18-24h.

The following day, synthesized MSNs were collected by centrifuging the reaction solution at 4500 rpm for 20 min. The obtained nanoparticle pellet was then washed with absolute ethanol twice to remove the excess reactants. CTAB in the nanoparticle pores was then removed with the solvent extraction method by using 1.2% (w/v) ammonium nitrate-absolute ethanol solution. The extraction process was carried out by stirring the MSNs in solvent extraction solution at 60°C for 12h. After that, products were collected by centrifugation at 10000 rpm and 4°C for 10 min and were washed with absolute ethanol several times. After performing the solvent extraction process once more, MSNs were either vacuum-dried and stored at room temperature or dispersed in DMF and kept at -20°C for further use.

2.2.2 Surface modification of MSNs

Surface chemistry of MSNs have been tuned by employing (3-aminopropyl)triethoxysilane (APTES) and succinic anhydride grafting in order to provide electrostatic interaction between MSN and BMP2-derived peptide at physiological pH 7 during the adsorption process. The first step of the surface modifications of MSNs were performed with amine anchoring groups which were required to achieve carboxyl modification for net negative surface charges to provide efficient electrostatic interaction and also re-dispersibility during the processes. To this end, MSNs at a concentration of 2.5 mg/mL were dispersed in toluene for 20 min using a sonication bath. Then, APTES solution at the ratio of 1:1 (µl APTES: mg nanoparticle) was pipetted into the mixture stirred at 450 rpm. The reaction was continued overnight at room temperature. The following day, toluene along with excess reactants were removed by centrifuging the solution at 12000 rpm for 10 min. MSNs-APTES were then washed with absolute ethanol and directly used for carboxyl modification.

After MSN-APTES was obtained, second step of the surface modification with succinic anhydride was performed. For this purpose, MSN-APTES (10 mg/ml) was first dispersed in DMF by sonication. Succinic anhydride (10.3 mg/ml) was then added to the nanoparticle solution during sonication. The mixture was stirred overnight at 410 rpm and room temperature. On the following day, the mixture was centrifuged at 12000 rpm for 10 min and the supernatant was discarded. Nanoparticle cake was washed with absolute ethanol twice, by sonication and centrifugation, subsequently. Carboxyl-modified MSNs was then dispersed in DMF and kept at -20^{o}C for further use.

2.2.3 Characterization of MSNs

2.2.3.1 Zeta potential and hydrodynamic size measurements

The hydrodynamic size and zeta potential of the MSNs were determined by dispersing MSNs in 4-(2-Hydroxyethyl)piperazine-1-ethanesulfonic acid (HEPES) buffer solution (pH=7.2, 25 mM) at the concentration of 0.25 mg/mL. Measurements were performed in triplicates using the Malvern Zetasizer instrument.

2.2.3.2 Nitrogen sorption analysis

Surface area (SA_{BET}), pore size (d_P), and pore volume (V_P) of the MSNs was determined by nitrogen sorption analysis using Micromeritics 3Flex instrument. The surface area of the MSNs was calculated using the Brunauer-Emmett-Teller (BET) theory. The analysis was performed by using approximately 200 mg of dried MSNs.

2.2.3.3 Scanning electron microscopy

SEM analysis of MSNs was performed in order to investigate the morphology and size of the synthesized materials. Approximately 100 µl of dispersed MSN solutions were spread onto glass coupons evenly and allowed to dry in a dust-free environment. On the following day, imaging was performed after sputtering all the samples with gold powder. During analysis, STEM (scanning transmission electron microscope) imaging was also carried out to visualize MSNs.

2.2.3.4 BMP2-derived peptide loading into MSNs

Loading of the BMP2-derived peptide into MSNs was performed in the presence of phosphate buffer (PB) (pH=7.2, 12 mM) solution. Briefly, BMP2 peptide stock solutions (10, 20, 50, 100 w/w% total weight of MSNs) pipetted into MSNs dispersed in PB while on the magnetic stirrer. Groups as the starting content of peptide to be used for loading degree determination was also prepared under the same conditions in the absence of MSNs. Thereafter, solutions were mixed at 400 rpm and room temperature for 1h to allow loading of the BMP2-derived peptide into MSNs pores. MSNs@BMP2 were then collected by centrifugation at 12000 rpm for 10 min. Supernatants were used to determine the amount of the BMP2-derived peptide remained in the solution. For that purpose, the absorbance of each supernatant was measured at 265 nm in triplicates in order to analyze the loading degree.

2.3 Synthesis and Characterization of PEGDMA Scaffolds

For hydrogel synthesis, PEGDMA at a concentration of 15% (w/v) was dispersed in phosphate-buffered saline (PBS) containing 0.5% (w/v) photoinitiator, 2-Hydroxy-4′-(2-hydroxyethoxy)-2-methylpropiophenone. After homogeneously dispersing the polymer precursor solution, photopolymerization using UV light was carried out. 30 µl of precursor solution was pipetted between a teflon mold and a glass slide, and 365 nm UV light at an intensity of 7 mW/cm^2 was applied for 2 min for complete polymerization of PEGDMA hydrogels.

2.3.1 Preparation of different hydrogel constructs

In this step, PEGDMA hydrogels incorporated with MSNs and HYAFF®11 polymer were fabricated. For optimization studies, PEGDMA hydrogel was embedded with MSNs at three different concentrations which were 0.25, 0.5, and 1% (w/w: MSNs/PEGDMA). After the determination of optimal MSNs concentration, HYAFF®11 polymer was incorporated into the hydrogel structure. For MSNs and HYAFF®11 incorporated PEGDMA hydrogel fabrication, the components were first dispersed in 0.5% photoinitiator solution separately and combined with PEGDMA polymer. The polymer precursor solution was then homogenized using a sonication bath to provide even distribution of the components. Polymerization of the MSNs-

PEGDMA, H-PEGDMA, or MSNs/H-PEGDMA was performed as described in Section 2.3.

2.3.2 Characterization of scaffolds

2.3.2.1 Compression test

During uniaxial compression tests, the effect of MSN and HYAFF®11 on the modulus of PEGDMA hydrogels was evaluated. Based on the preliminary results obtained for compression and swelling tests for scaffolds with different MSN concentrations, 1%MSN/1%HYAFF®11-PEGDMA (1MSN/1H-PEGDMA) and its counterparts PEGDMA, and 1%HYAFF®11-PEGDMA (1H-PEGDMA) were fabricated as described in Section 2.3.1 in the form of discs having 20 mm diameter and 1 mm thickness and taken for the compression analysis. After soaking the hydrogels in PBS for 24 h, the compression test was performed using a 20 mm parallel plate by subjecting the hydrogels to a crosshead speed of 10 µm/s at room temperature by using Discovery HR-2 hybrid rheometer. Compressive modulus for composite PEGDMA hydrogels was calculated by using the slope from the linear region (25-35% strain) of the obtained stress-strain curves.

2.3.2.2 Swelling test

The effect of the MSN and HYAFF®11 additives on swelling characteristics of the hydrogels was investigated through a swelling test. 1MSN/1H-PEGDMA and 1H-PEGDMA along with control PEGDMA hydrogel was fabricated as described previously. Later on, the hydrogels were incubated in PBS buffer at 37°C for 24h. After removal of PBS, excess liquid on hydrogel surfaces was eliminated and swollen weights (W_S) were measured. For determination of dry weight (W_D), the same hydrogels were vacuum dried at 60°C for 24h and weighed again. The percentage swelling of each hydrogel construct was calculated using the following equation (2.3.2.2), where Ws is the swollen and W_D is dried weight of the hydrogel samples.

$$Swelling\ (\%) = \left(\frac{W_S - W_D}{W_D}\right) \times 100 \qquad (2.1)$$

2.4 *In vitro* Cytocompatibility Assays

2.4.1 *In vitro* cytocompatibility of MSN constructs

In vitro biocompatibility of the synthesized MSNs, MSN@BMP2, and BMP2 peptide was evaluated in the L929 cell line (murine fibroblast cell line). L929 cells were maintained in Dulbecco's Modified Eagle Medium (DMEM) supplemented with 10% Fetal Bovine Serum (FBS) and 1% penicillin-streptomycin. For biocompatibility assay, L929 cells were seeded in 96 well plates at a density of 7000 cells/well and incubated at 37°C in 5% CO_2 environment for 24h to provide attachment of the cells. On the following day, media in the wells was replaced with fresh media containing different concentrations of MSNs, MSN@BMP2, or BMP2 corresponding to the amount loaded into the MSNs. Cells were then incubated at 37°C in 5% CO_2 incubator for 24 and 48h. After incubation with nanoparticles for defined time points, cell viability was assessed using alamarBlue™ Cell Viability Reagent (Invitrogen™, Thermo Fisher Scientific). For that purpose, alamarBlue solution (10% v/v) was directly added to the wells, and cells were incubated for another 4h in a dark environment. Fluorescence measurement was carried out at excitation/emission wavelength of 530/590 nm with CLARIOstar® plate reader to quantify resorufin product converted by metabolically active cells. In the experiment, non-treated cells were used as negative control while cells treated with 10% DMSO (v/v) were used as the positive control.

2.4.2 *In vitro* cytocompatibility of HYAFF®11

The effect of HYAFF®11 concentration on L929 cells were evaluated by using alamarBlue™ Cell Viability Reagent. For that purpose, L929 cells seeded at density of 7000 cells/ml were treated with fresh medium containing ascending concentrations (0.05, 1, and 2% w/v) of HYAFF®11 polymer. Treated cells were then incubated for 24 and 48h and cell viability were evaluated by using alamarBlue solution (10% v/v). Fluorescence quantification of reduced resorufin product was performed at excitation/emission wavelength of 530/590 nm. In the experiment, non-treated cells were used as negative control while cells treated with 10% DMSO (v/v) were used as the positive control.

2.4.3 *In vitro* cytocompatibility of PEGDMA, 1H-PEGDMA and 1MSN/1H-PEGDMA hydrogel scaffolds

In this step, the final form of the hydrogels, 1H-PEGDMA, 1MSN/1H-PEGDMA and PEGDMA were tested for their *in vitro* biocompatibility. For three-dimensional cell culture, cells were encapsulated within the scaffold matrix. For encapsulation of the cells, polymer precursor solutions were first prepared as described in Section 2.3.1. Then L929 cells at density of 5 x 10^6 cells/ml were mixed with precursor solutions directly before polymerization. 30 µl of cell-polymer mixture was then polymerized using 365 nm UV light at an intensity of 7 mW/cm^2 for 2 min. Cell encapsulated hydrogels were directly transferred into culture medium. The culture medium was replaced with a fresh medium after 1h in order to remove unreacted monomers. Afterwards, cell encapsulated scaffolds were incubated for 24, 48 and 72h. Cell viability was assessed by directly incubating the scaffolds with alamarBlue™ Cell Viability Reagent (10% v/v) for 4h in a dark environment. Fluorescence measurement was carried out at excitation/emission wavelength of 530/590 nm with CLARIOstar® plate reader to quantify resorufin product converted by viable cells.

2.5 Statistical Analysis

The experiments were carried out in triplicates and Graphpad Prism software (Version 8.4.2) was used for statistical analysis. Data are represented as mean ± standard deviation (SD) and level of significance (α) was set to 0.05.

3. RESULTS AND DISCUSSION

3.1 Synthesis and Characterization of MSNs

Conventional MSNs usually have pore size of approximately 3 nm which is insufficient for large biomolecule delivery, such as proteins and peptides, for therapeutic applications. For delivery of such biomolecules, synthesis of MSNs with large mesopores, i.e. >5 nm, with uniform particle size is required. To this end, one of the approaches is to utilize pore expanding agents such as long-chain alkanes during synthesis or pore swelling agents such as trimethylbenzene or decane post-synthesis [47–49]. However, these methods often results in distorted pore structure and changes in nanoparticle size which eventually led to development of new methods for large pore MSN synthesis. During studies, a recently new method based on water-oil biphase stratification has been exploited for synthesis of MSNs to achieve high loading capacity of BMP2-derived peptide [46]. This method enables one-pot fabrication of large pore MSNs by simply employing organic solvents of different hydrophobicity and molecular size which results in tunable swelling behavior and hence mesopore size (Figure 3.1).

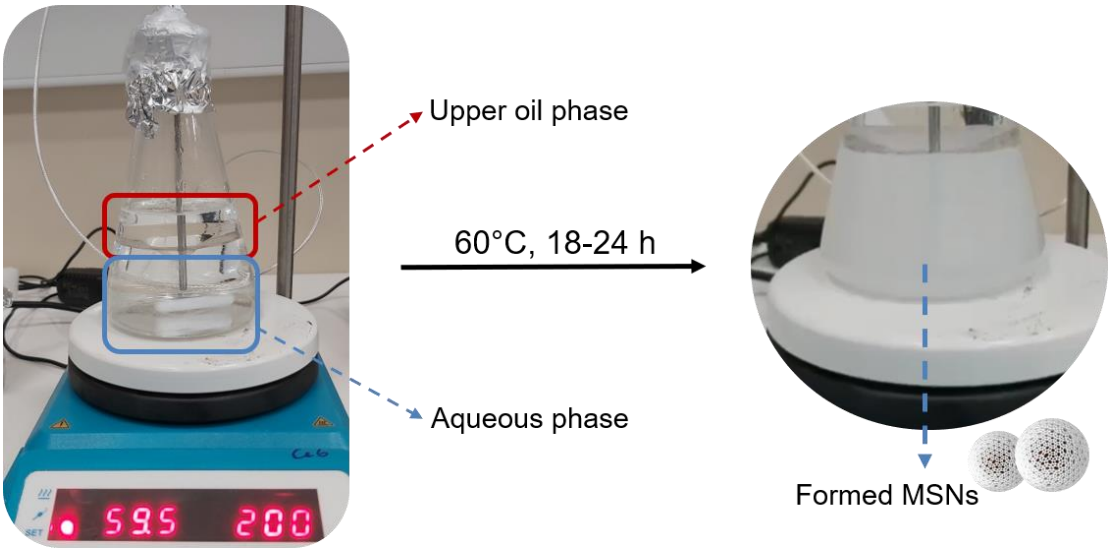

Figure 3.1 Synthesis of MSNs with large pores by employing water-oil biphase stratification reaction.

Concentration of TEOS in the oil phase is also a determining factor affecting pore size in terms of silica source availability. By taking these parameters into consideration,

MSNs with various concentrations of TEOS (5, 10, 20% v/v) and cyclohexane being the organic solvent were synthesized at initial studies and MSN with 20% (v/v) concentration was shown to demonstrate best morphology according to SEM analysis (data not shown). Therefore, rest of the studies, BMP2-derived peptide loading and hydrogel construction, was performed with the optimized MSN.

During characterization studies, SEM and STEM imaging were employed to investigate morphology, size and monodispersity of the MSNs. As shown in Figure 3.2.A, spherical MSNs with diameters of around 150 nm is successfully synthesized. Monodispersibility of MSNs were also revealed with SEM imaging which is an indication for narrow size distribution. On the other hand, STEM micrograph (Figure 3.2.B) shows dendrimer-like porous architecture of MSNs specifically near the surface which may be due to presence of large pores.

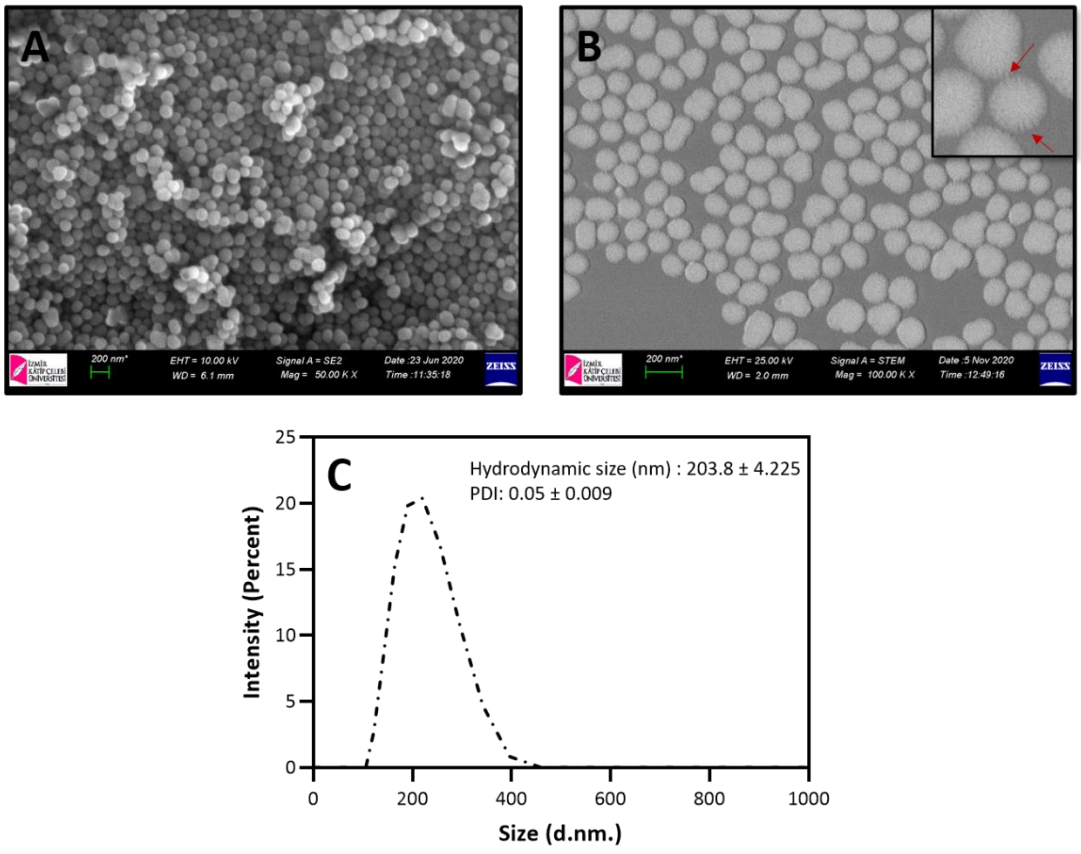

Figure 3.2 A) SEM image, **B)** STEM image and **C)** hydrodynamic size distribution of MSNs. Inset figure shows large mesopore openings at the surface of MSNs.

The size of MSNs was also analyzed by employing DLS technique. According to results, hydrodynamic diameter of MSN is around 200 nm (Figure 3.2.C) with a polydispersity index (PDI) value of 0.05. PDI is a measure of size uniformity of the nanoparticle and samples having PDI value below 0.08 are considered to be monodisperse as observed in MSN samples (Table 3.1). The difference in the size of MSNs obtained from SEM and DLS techniques is a situation normally encountered in nanoparticle analyses because SEM analysis provide dry nanoparticle size, whereas DLS technique measures size of the nanoparticles plus solvent layer formed around [50].

Net surface charge of carboxyl group modified-MSNs at neutral pH was determined by ζ-potential measurements. ζ-potential value of MSNs was found to be -29.3 mV demonstrating colloidal dispersion stability of the synthesized nanoparticles (Table 3.1). Since pure MSNs without any surface modification generally have ζ-potential value of around -6 mV, the obtained result also proves successful surface modification of the MSNs with succinic anhydride which results in negative surface charge due to the formation of carboxyl groups as demonstrated in Figure 3.3. Surface modification was employed to provide electrostatic interaction between MSN and BMP2-derived peptide during peptide loading studies in order to obtain a high loading degree.

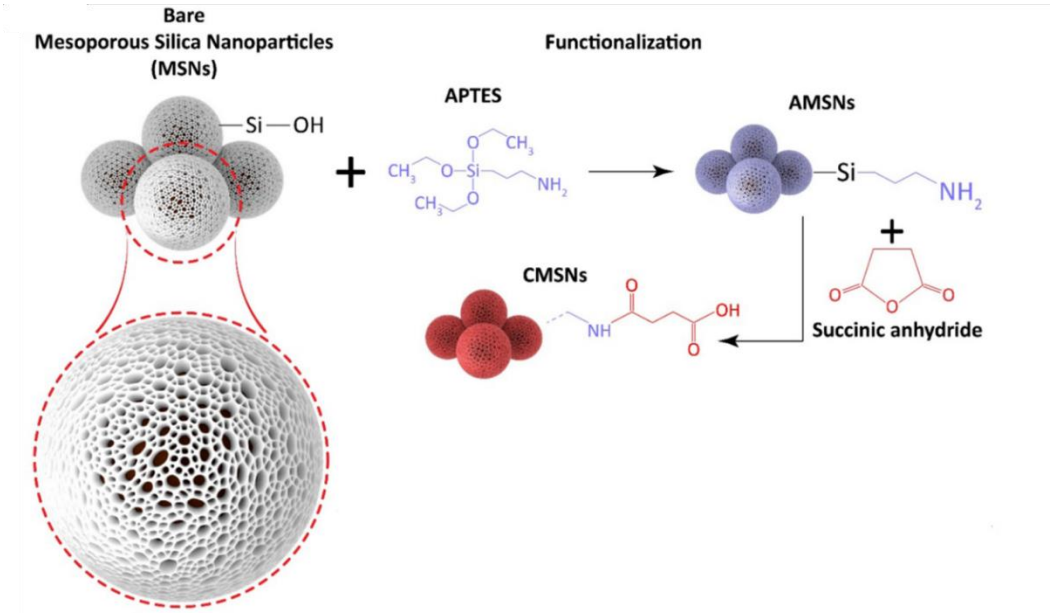

Figure 3.3 Demonstration of chemical modifications to produce surface-functionalized MSNs. Figure is adapted from [51].

Table 3.1 Size, net surface charge and surface area values of MSNs.

Characterization	Result
Hydrodynamic size (nm)	203.8 ± 4.225
PDI	0.05 ± 0.009
ζ-Potential value (mV)	-29.3 ± 2.37
BET surface area (m^2/g)	668.3059
Pore size (nm)	8.8

Nitrogen sorption analysis was further carried out to measure pore diameter and specific surface area of the MSNs according to the BET theory. As shown in Figure 3.4, MSNs have an average pore size of 8.8 nm with specific surface area of 668 m^2/g. This results demonstrate that synthesized MSNs are suitable carriers for efficient loading, delivery and preserving of bioactive molecules, in this case, BMP2-derived peptide.

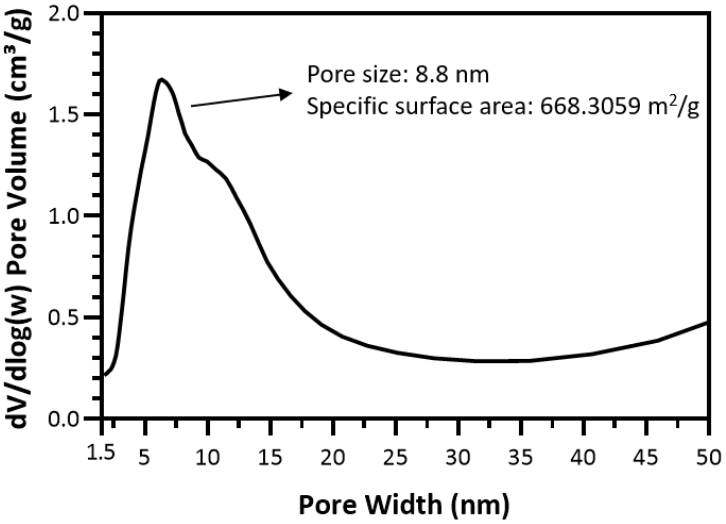

Figure 3.4 Pore size distribution of MSNs.

As a model bioactive molecule, BMP2-derived peptide, having amino acid sequence of KIPKASSVPTELSAISTLY corresponding to 73-92 residues of BMP2 protein, was synthesized based on the solid-phase peptide synthesis chemistry. The obtained peptide has isoelectric point of 9.7 with the estimated molecular weight of 2118.50 g/mol. Since synthesized peptide has a hydrophobic nature due to the non-polar and polar uncharged amino acids in its structure, utilization of MSNs as carrier systems is favorable. BMP2-derived peptide loading into MSNs was carried out at neutral pH

(pH 7.2, 12 mM phosphate buffer) at which both MSNs and peptide become oppositely charged to facilitate electrostatic interaction. BMP2-derived peptide was loaded in 4 different concentrations corresponding to total MSN weight (w/w%) to investigate loading ability. As demonstrated in Table 3.2, the loading with highest degree of 70% was achieved with concentration of 100% (w/w).

Table 3.2 Initial loading degree of BMP2-derived peptide with respect to mass of MSNs and obtained loading degree results.

Initial Degree (w/w%)	Loaded Degree (%)
10	4.07
20	13.95
50	30.37
100	70

3.2 Fabrication and Characterization of Scaffolds

After evaluation of physicochemical properties and *in vitro* biocompatibility of the MSNs, BMP2-derived peptide and HYAFF®11, PEGDMA hydrogel scaffolds embedded with these components were fabricated. Initial studies were first carried out for PEGDMA hydrogels embedded with 0.25, 0.5 and 1% MSN (w/w) in order to determine optimal nanoparticle concentration. According to preliminary results (Appendix 1), 1MSN-PEGDMA showed optimal characteristics and therefore used in combination with HYAFF®11 for the rest of the study. For the following characterization studies, PEGDMA, 1H-PEGDMA and 1MSN/1H-PEGDMA hydrogels were crosslinked by employing photopolymerization. MSN or HYAFF®11 was added to polymer precursor solution comprising PEGDMA and photoinitiator, and thoroughly dispersed just before UV treatment to provide even distribution of the MSN and HYAFF®11 within the polymer network of PEGDMA. A representative image of polymerized hydrogels containing 1% MSN (w/w) and 1% HYAFF®11 (w/w) is shown in Figure 3.5.

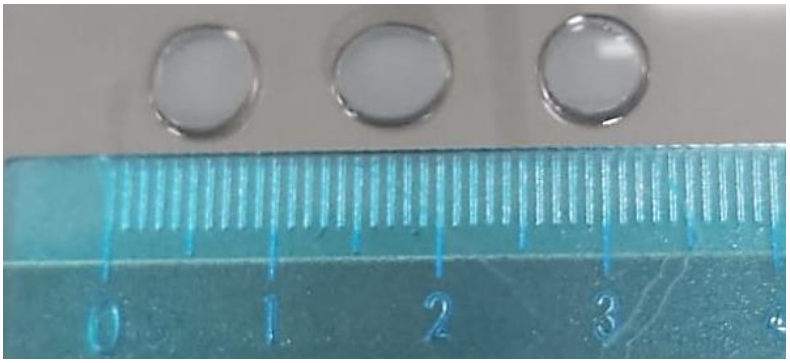

Figure 3.5 Images of 1MSN/1H-PEGDMA hydrogels employed for cell encapsulation studies.

The combination of MSNs with PEG-derived polymers has taken part in literature to enhance some features such as cell adhesion or mechanical properties of hydrogels. Zhan et al. used PEGDA hydrogels embedded with 20 nm sized silica nanoparticles to investigate the effect of the particles on viscoelastic behavior of the fabricated hydrogels. Authors showed that viscoelastic properties of the silica nanoparticle-polymer interphase differs from the viscoelastic behavior of the pure polymer even at small concentrations of silica nanoparticles [52]. Therefore, the effect of MSN and HYAFF®11 on PEGDMA hydrogels was investigated with compression and swelling test to determine whether these components result in a dramatic change in comparison to pure PEGDMA hydrogel. Hydrogels prepared in the disc form were first subjected to compression testing to evaluate the response of the gels to increasing compressive force. As shown in Figure 3.6, stress-strain curve obtained for PEGDMA and 1H-PEGDMA hydrogel scaffolds are similar to each other. When MSN is further embedded to 1H-PEGDMA hydrogel, a slight decrease in the strain revealing increased resistance to deformation was observed. Hocken et al stated that presence of the MSNs in polymer solution during crosslinking step prevents complete formation of polymer network in comparison to pure PEGDMA hydrogels. This has resulted in a PEGDMA hydrogel with higher crosslink density leading to a stronger response to compression than 1MSN/1H-PEGDMA hydrogels [53].

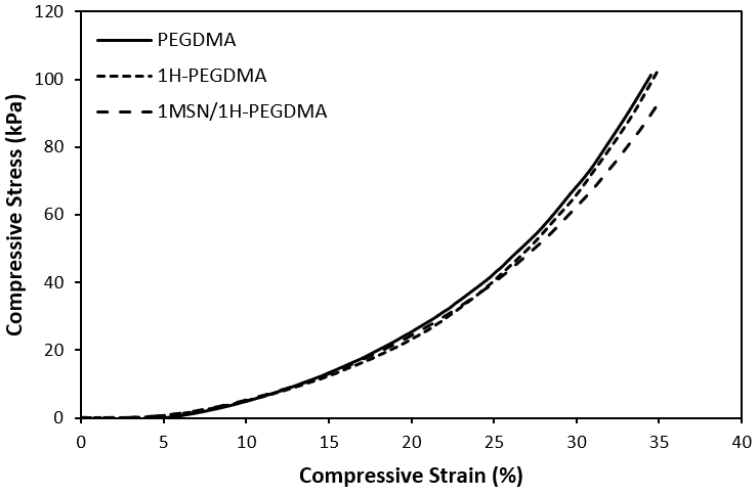

Figure 3.6 Compressive stress vs. strain graph of hydrogel scaffolds with different compositions.

The obtained stress-strain curves were then used to determine compressive modulus of PEGDMA, 1H-PEGDMA and 1MSN/1H-PEGDMA hydrogels by calculating the slope from the linear region of the curves. Although a slight decrease in the compressive modulus of 1MSN/1H-PEGDMA hydrogel is observed, no significant difference between PEGDMA and 1MSN/1H-PEGDMA hydrogels was determined as demonstrated in Figure 3.7.

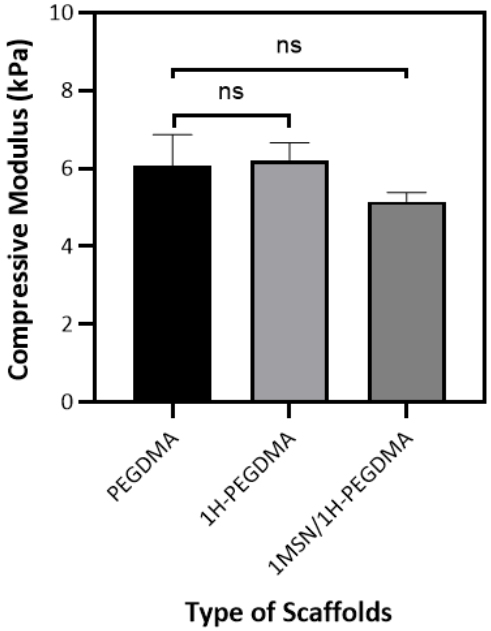

Figure 3.7 Compressive moduli of scaffolds. Statistical analysis of compressive modulus was performed with respect to PEGDMA by applying ordinary one-way ANOVA followed by Tukey's multiple comparisons test. ns: non-significant.

Swelling tests were performed for same groups as in compression test, which are PEGDMA, 1H-PEGDMA and 1MSN/1H-PEGDMA hydrogel scaffolds. According to results, presence of the MSN and HYAFF®11 in the PEGDMA polymer network resulted in a slight decrease in the swelling ability when compared to pure PEGDMA hydrogels (Figure 3.8). On the other hand, no significant difference between swelling behavior of PEGDMA and 1H-PEGDMA was observed. Therefore, the decline observed in swelling of 1MSN/1H-PEGDMA hydrogel scaffold could be attributed to existence of MSNs. Gaharwar et al also showed that swelling degree of PEGDA hydrogels has decreased as the silica nanoparticle concentration in the polymer network increased [54]. When hydrogels are embedded with nanoparticles, either interaction between nanoparticles and polymer chains could prevent complete polymerization or nanoparticles could restrict chain movement of polymer network, which eventually results in decreased swelling behavior. These findings correlate with the compressive moduli results in which an insignificant decrease in the compressive modulus for 1MSN/1H-PEGDMA was observed.

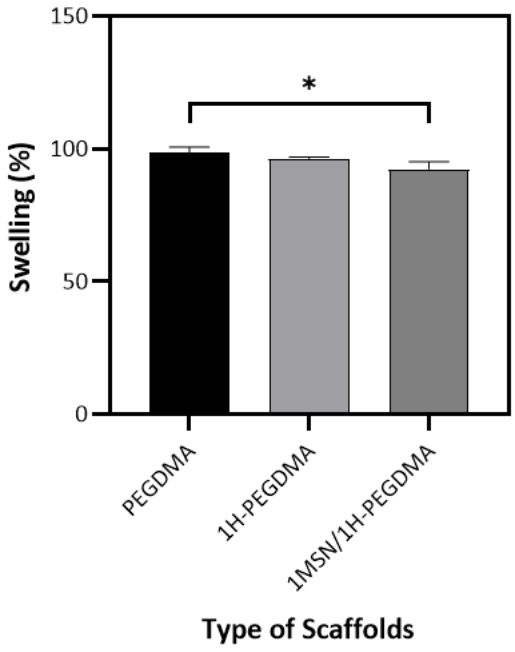

Figure 3.8 Swelling characteristics of scaffolds embedded with MSN and/or HYAFF®11 polymer. Statistical analysis of swelling test was performed with respect to PEGDMA by applying ordinary one-way ANOVA followed by Tukey's multiple comparisons test. The level of significance was *$p<0.05$.

3.3 *In vitro* Cytocompatibility Assays

The *in vitro* cytocompatibility of the pristine MSNs, MSN@BMP2-derived peptide, and BMP2-derived peptide alone was evaluated on L929 cell line at ascending concentrations to determine the safe range for the following applications. Concentrations of BMP2-derived peptide was determined according to the amount loaded into MSNs determined by UV visible spectroscopy. Cell viability was assessed with alamarBlue™ Cell Viability Reagent (Invitrogen™, Thermo Fisher Scientific), which is a ready-to-use solution containing the active ingredient resazurin. Resazurin is a non-toxic, cell permeable and non-fluorescent chemical. After uptake by living cells, resazurin is reduced to a highly fluorescent product, resorufin, that enables sensitive quantification of cell viability and proliferation. As demonstrated in Figure 3.9.A, pristine MSN is not cytotoxic to cells even at high concentrations as 100 µg/ml at both 24 and 48h. MSN@BMP2-derived peptide also does not decrease cell viability (Figure 3.9.B). On the other hand, BMP2-derived peptide increased cell viability significantly at 31 and 62 µg/ml. Therefore, MSN@BMP2 with 100% (w/w) peptide loading was chosen for the following studies. In addition to this, cell viability data was used to determine the MSN concentration to be incorporated into the PEGDMA scaffolds.

During experiments, *in vitro* toxicity of HYAFF®11 was also investigated to determine the non-toxic concentration to embed into PEGDMA hydrogel scaffolds. *In vitro* tests for HYAFF®11 polymer were carried on L929 cells under the same test conditions performed for nanoparticle groups. Cells were exposed to 0.05, 1 and 2% (w/v) HYAFF®11 for different culture time points, and cell viability was quantified by alamarBlue™ Cell Viability Reagent. As in Figure 3.10, results showed that HYAFF®11 is biocompatible at all concentrations. Moreover, 1% (w/v) HYAFF®11 showed highest cell viability at 24h. Since the compound of the HYAFF®11 is hyaluronic acid, which is naturally found in the ECM of tissues, it is expected to obtain a three-dimensional environment that mimicking the behaviour of the natural ECM after incorporation of the HYAFF®11 into the PEGDMA hydrogel scaffolds.

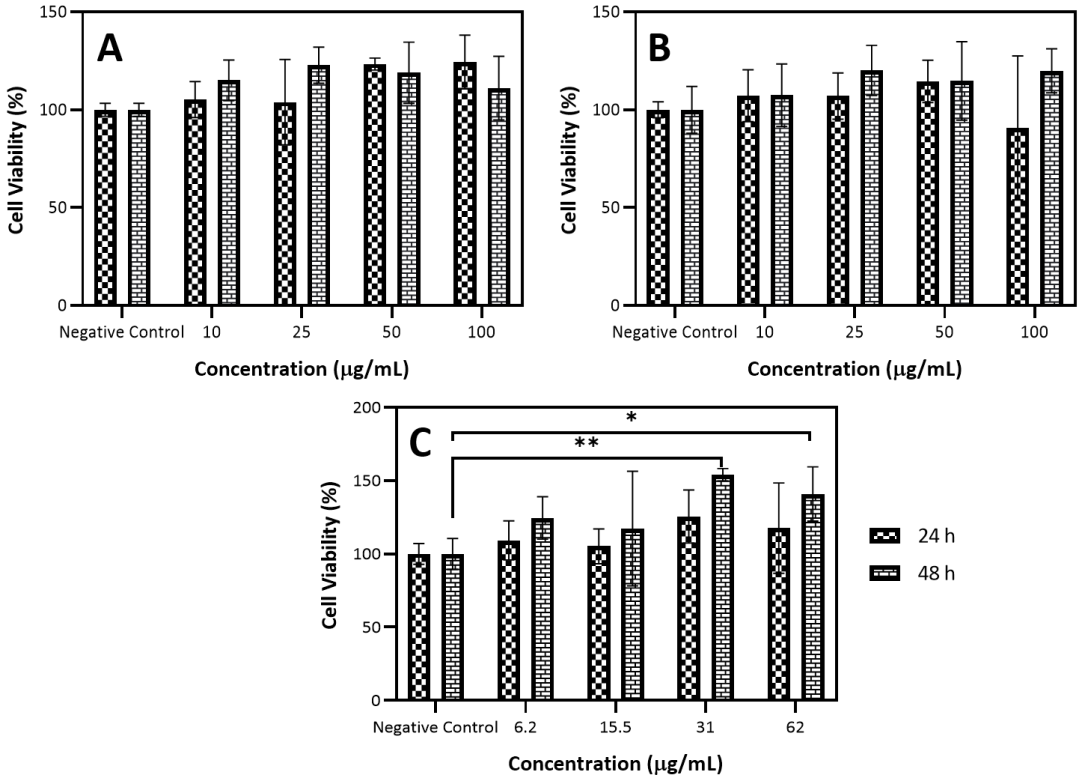

Figure 3.9 Viability analysis of L929 cell line after exposure to different concentrations of **A)** pristine MSN, **B)** MSN@BMP-2 derived peptide **C)** BMP2-derived peptide alone. Statistical analysis of cell viability with respect to negative control was performed by applying ordinary two-way ANOVA followed by Dunnett's multiple comparison test with significance level of *p<0.05 and **p<0.01.

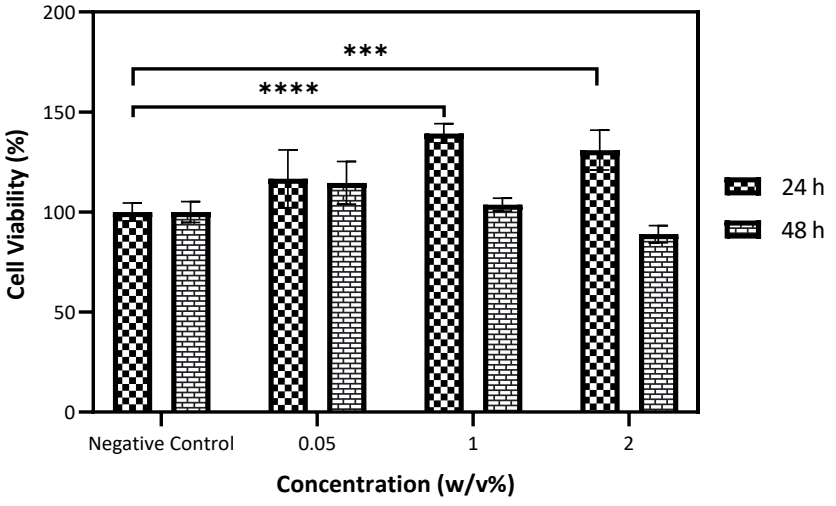

Figure 3.10 Cell viability analysis of HYAFF®11 polymer. Statistical analysis was performed with respect to negative control using ordinary two-way ANOVA followed by Dunnett's multiple comparison test with significance level of ***p<0.001, ****p<0.0001.

After demonstration of biocompatibility of MSN constructs and HYAFF®11, these additives were combined with PEGDMA hydrogel to fabricate scaffolds for encapsulation of L929 cells. The response of cells to three-dimensional culture environment was then assessed with viability assays. To this end, cells were mixed with polymer precursor solutions and thereafter exposed to UV light to achieve polymerization. After 24, 48 and 72h, metabolically active cells were quantified using alamarBlue™ Cell Viability Reagent. During analysis, 1H-PEGDMA and 1MSN/1H-PEGDMA were compared to pure PEGDMA scaffold to evaluate the effects of these additives on cells. As shown in Figure 3.11, 1H-PEGDMA and 1MSN/1H-PEGDMA did not generally show a cytotoxic effect against cells. Besides, 1MSN/1H-PEGDMA scaffolds shows good compatibility with cells at 24h. In addition, the impact of MSN presence at different level of concentrations were also evaluated as presented in Appendix 2. During analysis, it was also observed that non-crosslinked polymer precursor solution could show a toxic effect to cells to some extent which may lead to an insignificant decrease in the cell viability.

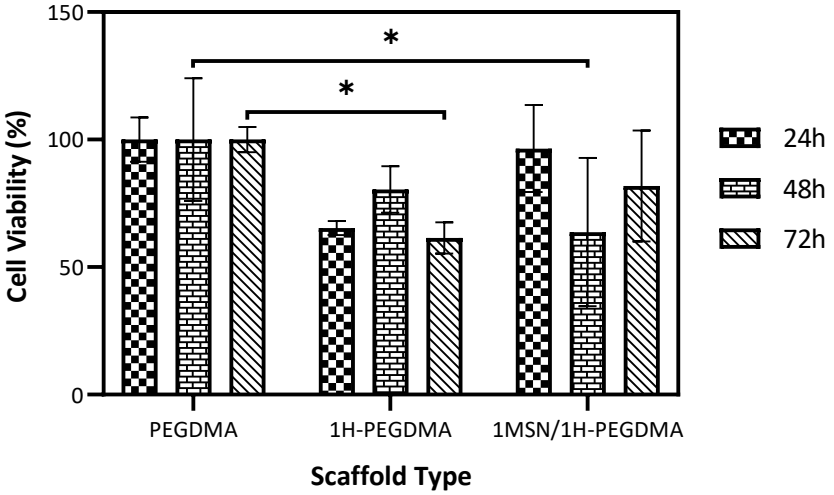

Figure 3.11 Viability analysis of cell encapsulated PEGDMA, 1H-PEGDMA, and 1MSN/1H-PEGDMA scaffolds. Statistical analysis was performed with respect to PEGDMA scaffolds using ordinary two-way ANOVA followed by Dunnett's multiple comparison test with significance level of *$p<0.05$.

4. CONCLUSION

In this study, PEGDMA hydrogels with multi-functionality were fabricated and analyzed for their potential in various tissue engineering applications. The motivation behind this study is that even though PEGDMA hydrogel provides an inert environment for the cells, it does not promote cell adhesion and proliferation when used as a scaffold. Insufficient cell adhesion could be improved by incorporation of polymers of natural origin into the hydrogel structure. Cell proliferation and differentiation could be further induced by presentation of small bioactive molecules to cells in the hydrogels. However, diffusion followed by requirement for administration of high doses of these molecules reduces its effectiveness. To overcome this problem, nanoparticles could be combined with scaffolds to provide controlled delivery and release of bioactive molecules. Those two strategies are combined in this study to develop a three-dimensional scaffold with improved characteristics. To this end, HYAFF®11, hyaluronic acid benzyl ester, was incorporated into PEGDMA polymer to increase biocompatibility while BMP2-derived peptide loaded MSNs was used to enhance differentiation and proliferation of the cells. MSNs with large pores, 8.8 nm, was synthesized in the initial stages of the thesis and well characterized with various characterization techniques. Thereafter, BMP-2 derived peptide was loaded into the pores of MSNs by employing electrostatic interactions which led to a high degree of loading. PEGDMA hydrogels were then embedded with MSN and HYAFF®11 to fabricate composite hydrogels, 1H-PEGDMA and 1MSN/1H-PEGDMA. The effect of embedded components on the mechanical and swelling performance of the hydrogels in comparison to pure PEGDMA hydrogel was then investigated. Results demonstrated that incorporation of HYAFF®11 did not alter the compression modulus or swelling performance of the PEGDMA hydrogels. When MSNs were included in 1H-PEGDMA network, a slight decrease in compressive modulus and swelling performance was observed as expected. In the final step, the viability of the L929 cells when cultured within PEGDMA, 1H-PEGDMA and 1MSN/1H-PEGDMA scaffolds were evaluated. Results showed that the developed multifunctional hydrogels do not show toxicity against cells and provide a bio-mimicking environment for three-dimensional culturing. Taken together, this study

demonstrates that multifunctional scaffolds could be developed by the use of MSNs. The obtained results will be further supported by encapsulation of mesenchymal stem cells within 1MSN@BMP-2/1H-PEGDMA scaffolds to induce osteogenic differentiation.

REFERENCES

1. Parra-Torres AY, Valdés-Flores M, Velázquez-Cruz LO and R. Molecular Aspects of Bone Remodeling. Topics in Osteoporosis [Internet]. 2013 May 15 [cited 2021 Jan 3].

2. J Hill M, Qi B, Bayaniahangar R, Araban V, Bakhtiary Z, Doschak MR, et al. Nanomaterials for bone tissue regeneration: updates and future perspectives. Nanomedicine. 2019;14(22):2987–3006.

3. Toosi S, Behravan J. Osteogenesis and bone remodeling: A focus on growth factors and bioactive peptides. BioFactors. 2020;46(3):326–40.

4. Wu M, Chen G, Li Y-P. TGF-β and BMP signaling in osteoblast, skeletal development, and bone formation, homeostasis and disease. Bone Res. 2016;4(1):16009.

5. Rivera JC, Strohbach CA, Wenke JC, Rathbone CR. Beyond osteogenesis: an in vitro comparison of the potentials of six bone morphogenetic proteins. Front Pharmacol [Internet]. 2013 [cited 2021 Jan 3].

6. Zhang X, Guo W-G, Cui H, Liu H-Y, Zhang Y, Müller WEG, et al. In vitro and in vivo enhancement of osteogenic capacity in a synthetic BMP-2 derived peptide-coated mineralized collagen composite. J Tissue Eng Regen Med. 2016;10(2):99–107.

7. Yang J, Shi P, Tu M, Wang Y, Liu M, Fan F, et al. Bone morphogenetic proteins: Relationship between molecular structure and their osteogenic activity. Food Science and Human Wellness. 2014;3(3–4):127–35.

8. Katagiri T, Watabe T. Bone Morphogenetic Proteins. Cold Spring Harb Perspect Biol. 2016;8(6):a021899.

9. Migliorini E, Valat A, Picart C, Cavalcanti-Adam EA. Tuning cellular responses to BMP-2 with material surfaces. Cytokine & Growth Factor Reviews. 2016;27:43–54.

10. Mohammadi M, Mousavi Shaegh SA, Alibolandi M, Ebrahimzadeh MH, Tamayol A, Jaafari MR, et al. Micro and nanotechnologies for bone regeneration: Recent advances and emerging designs. J Control Release. 2018;274:35–55.

11. Park JY, Park SH, Kim MG, Park S-H, Yoo TH, Kim MS. Biomimetic Scaffolds for Bone Tissue Engineering. In: Noh I, editor. Biomimetic Medical Materials: From Nanotechnology to 3D Bioprinting. Singapore: Springer; 2018;p. 109–21.

12. Burke G, Barron V, Geever T, Geever L, Devine DM, Higginbotham CL. Evaluation of the materials properties, stability and cell response of a range of PEGDMA hydrogels for tissue engineering applications. Journal of the Mechanical Behavior of Biomedical Materials. 2019;99:1–10.

13. Tan F, Liu J, Liu M, Wang J. Charge density is more important than charge polarity in enhancing osteoblast-like cell attachment on poly(ethylene glycol)-diacrylate hydrogel. Materials Science and Engineering: C. 2017;76:330–9.

14. Ingavle GC, Gehrke SH, Detamore MS. The bioactivity of agarose–PEGDA interpenetrating network hydrogels with covalently immobilized RGD peptides and physically entrapped aggrecan. Biomaterials. 2014;35(11):3558–70.

15. Amorim S. Extracellular Matrix Mimics Using Hyaluronan-Based Biomaterials. Trends in Biotechnology. 2020;39(1):90-104.

16. Fallacara A, Baldini E, Manfredini S, Vertuani S. Hyaluronic Acid in the Third Millennium. Polymers. 2018;10(7):701.

17. Zhu Z, Wang Y-M, Yang J, Luo X-S. Hyaluronic acid: a versatile biomaterial in tissue engineering. PAR. 2017;4(12):219.

18. Bauer C, Berger M, Baumgartner RR, Höller S, Zwickl H, Niculescu-Morzsa E, et al. A Novel Cross-Linked Hyaluronic Acid Porous Scaffold for Cartilage Repair: An In Vitro Study With Osteoarthritic Chondrocytes. Cartilage. 2016;7(3):265–73.

19. Pluda S, Pavan M, Galesso D, Guarise C. Hyaluronic acid auto-crosslinked polymer (ACP): Reaction monitoring, process investigation and hyaluronidase stability. Carbohydrate Research. 2016;433:47–53.

20. Brittberg M. Knee Cartilage Repair with Hyalograft® (Hyaff-11 Scaffold with Seeded Autologous Chondrocytes). In: ESSKA ASBL, Shetty AA, Kim S-J, Nakamura N, Brittberg M, editors. Techniques in Cartilage Repair Surgery [Internet]. Berlin, Heidelberg: Springer Berlin Heidelberg; 2014;p. 227–35.

21. Mermerkaya MU, Doral MN, Karaaslan F, Huri G, Karacavuş S, Kaymaz B, et al. Scintigraphic evaluation of the osteoblastic activity of rabbit tibial defects after HYAFF11 membrane application. J Orthop Surg Res. 2016;11(1):57.

22. Skaalure SC, Dimson SO, Pennington AM, Bryant SJ. Semi-interpenetrating networks of hyaluronic acid in degradable PEG hydrogels for cartilage tissue engineering. Acta Biomater. 2014;10(8):3409–20.

23. Madl CM, Mehta M, Duda GN, Heilshorn SC, Mooney DJ. Presentation of BMP-2 Mimicking Peptides in 3D Hydrogels Directs Cell Fate Commitment in Osteoblasts and Mesenchymal Stem Cells. Biomacromolecules. 201;15(2):445–55.

24. Falcigno L, D'Auria G, Calvanese L, Marasco D, Iacobelli R, Scognamiglio PL, et al. Osteogenic properties of a short BMP-2 chimera peptide. Journal of Peptide Science. 2015;21(9):700–9.

25. Baumann B, Jungst T, Stichler S, Feineis S, Wiltschka O, Kuhlmann M, et al. Control of Nanoparticle Release Kinetics from 3D Printed Hydrogel Scaffolds. Angew Chem Int Ed. 2017;56(16):4623–8.

26. Mohammadi M, Mousavi Shaegh SA, Alibolandi M, Ebrahimzadeh MH, Tamayol A, Jaafari MR, et al. Micro and nanotechnologies for bone regeneration: Recent advances and emerging designs. Journal of Controlled Release. 2018;274:35–55.

27. Zouani OF, Kalisky J, Ibarboure E, Durrieu MC. Effect of BMP-2 from matrices of different stiffnesses for the modulation of stem cell fate. Biomaterials. 2013;34(9):2157–66.

28. Chen Y, Liu X, Liu R, Gong Y, Wang M, Huang Q, et al. Zero-order controlled release of BMP2-derived peptide P24 from the chitosan scaffold by chemical grafting modification technique for promotion of osteogenesis *in* vitro and enhancement of bone repair *in vivo*. Theranostics. 2017;7(5):1072–87.

29. Mohammadi M, Alibolandi M, Abnous K, Salmasi Z, Jaafari MR, Ramezani M. Fabrication of hybrid scaffold based on hydroxyapatite-biodegradable nanofibers incorporated with liposomal formulation of BMP-2 peptide for bone tissue engineering. Nanomedicine: Nanotechnology, Biology and Medicine. 2018;14(7):1987–97.

30. Mercado AE, Yang X, He X, Jabbari E. Effect of Grafting BMP2 Derived Peptide to Nanoparticles on Osteogenic and Vasculogenic Expression of Stromal Cells. J Tissue Eng Regen Med. 2014;8(1):15–28.

31. Jabbari E, Mercado AE, Ma J, He X. Effect of BMP-2 Derived Peptide Grafted to Nanoparticles on Differentiation of Stromal Cells. MRS Online Proceedings Library (OPL) [Internet]. 2012 ed [cited 2021 Jan 2];1417.

32. Sansanaphongpricha K, Sonthithai P, Kaewkong P, Thavornyutikarn B, Bamrungsap S, Kosorn W, et al. Hyaluronic acid-coated gold nanorods enhancing BMP-2 peptide delivery for chondrogenesis. Nanotechnology. 2020;31(43):435101.

33. Bagheri E, Ansari L, Abnous K, Taghdisi SM, Charbgoo F, Ramezani M, et al. Silica based hybrid materials for drug delivery and bioimaging. Journal of Controlled Release. 2018;277:57–76.

34. Darouie S, Ansari Majd S, Rahimi F, Hashemi E, Kabirsalmani M, Dolatshahi-Pirouz A, et al. The fate of mesenchymal stem cells is greatly influenced by the surface chemistry of silica nanoparticles in 3D hydrogel-based culture systems. Materials Science and Engineering: C. 2020;106:110259.

35. Andrée L, Barata D, Sutthavas P, Habibovic P, van Rijt S. Guiding mesenchymal stem cell differentiation using mesoporous silica nanoparticle-based films. Acta Biomaterialia. 2019;96:557–67.

36. Eivazzadeh-Keihan R, Chenab KK, Taheri-Ledari R, Mosafer J, Hashemi SM, Mokhtarzadeh A, et al. Recent advances in the application of mesoporous silica-based nanomaterials for bone tissue engineering. Materials Science and Engineering: C. 2020;107:110267.

37. Rosenholm JM, Zhang J, Linden M, Sahlgren C. Mesoporous silica nanoparticles in tissue engineering--a perspective. Nanomedicine (Lond). 2016;11(4):391–402.

38. Zhou X, Feng W, Qiu K, Chen L, Wang W, Nie W, et al. BMP-2 Derived Peptide and Dexamethasone Incorporated Mesoporous Silica Nanoparticles for Enhanced Osteogenic Differentiation of Bone Mesenchymal Stem Cells. ACS Appl Mater Interfaces. 2015;7(29):15777–89.

39. Chen L, Zhou X, He C. Mesoporous silica nanoparticles for tissue-engineering applications. Wiley Interdiscip Rev Nanomed Nanobiotechnol. 2019;11(6):e1573.

40. Cui W, Liu Q, Yang L, Wang K, Sun T, Ji Y, et al. Sustained Delivery of BMP-2-Related Peptide from the True Bone Ceramics/Hollow Mesoporous Silica Nanoparticles Scaffold for Bone Tissue Regeneration. ACS Biomater Sci Eng. 2018;4(1):211–21.

41. Yao Q, Liu Y, Selvaratnam B, Koodali RT, Sun H. Mesoporous silicate nanoparticles/3D nanofibrous scaffold-mediated dual-drug delivery for bone tissue engineering. Journal of Controlled Release. 2018;279:69–78.

42. Killion JA, Geever LM, Devine DM, Kennedy JE, Higginbotham CL. Mechanical properties and thermal behaviour of PEGDMA hydrogels for potential bone regeneration application. Journal of the Mechanical Behavior of Biomedical Materials. 2011;4(7):1219–27.

43. Jiang T, Zhao J, Yu S, Mao Z, Gao C, Zhu Y, et al. Untangling the response of bone tumor cells and bone forming cells to matrix stiffness and adhesion ligand density by means of hydrogels. Biomaterials. 2019;188:130–43.

44. Bhakta G, Rai B, Lim ZXH, Hui JH, Stein GS, van Wijnen AJ, et al. Hyaluronic acid-based hydrogels functionalized with heparin that support controlled release of bioactive BMP-2. Biomaterials. 2012;33(26):6113–22.

45. Xu C, Xiao L, Cao Y, He Y, Lei C, Xiao Y, et al. Mesoporous silica rods with cone shaped pores modulate inflammation and deliver BMP-2 for bone regeneration. Nano Res. 2020;13(9):2323–31.

46. Shen D, Yang J, Li X, Zhou L, Zhang R, Li W, et al. Biphase stratification approach to three-dimensional dendritic biodegradable mesoporous silica nanospheres. Nano Lett. 2014;14(2):923–32.

47. Kao K-C, Mou C-Y. Pore-expanded mesoporous silica nanoparticles with alkanes/ethanol as pore expanding agent. Microporous and Mesoporous Materials. 2013;169:7–15.

48. Na H-K, Kim M-H, Park K, Ryoo S-R, Lee KE, Jeon H, et al. Efficient Functional Delivery of siRNA using Mesoporous Silica Nanoparticles with Ultralarge Pores. Small. 2012;8(11):1752–61.

49. Fuertes AB, Valle-Vigón P, Sevilla M. Synthesis of colloidal silica nanoparticles of a tunable mesopore size and their application to the adsorption of biomolecules. Journal of Colloid and Interface Science. 2010;349(1):173–80.

50. Kaasalainen M, Aseyev V, von Haartman E, Karaman DŞ, Mäkilä E, Tenhu H, et al. Size, Stability, and Porosity of Mesoporous Nanoparticles Characterized with Light Scattering. Nanoscale Res Lett. 2017;12(1):74.

51. Hasany M, Taebnia N, Yaghmaei S, Shahbazi M-A, Mehrali M, Dolatshahi-Pirouz A, et al. Silica nanoparticle surface chemistry: An important trait affecting cellular biocompatibility in two and three dimensional culture systems. Colloids and Surfaces B: Biointerfaces. 2019;182:110353.

52. Zhan Y, Pan Y, Chen B, Lu J, Zhong Z, Niu X. Strain rate dependent hyperelastic stress-stretch behavior of a silica nanoparticle reinforced poly (ethylene glycol) diacrylate nanocomposite hydrogel. Journal of the Mechanical Behavior of Biomedical Materials. 2017;75:236–43.

53. Hocken A, Yang Y, Beyer FL, Morgan BF, Kline K, Piper T, et al. Photocurable Poly(ethylene glycol) Diacrylate Resins with Variable Silica Nanoparticle Loading. Ind Eng Chem Res. 2019;58(32):14775–84.

54. Gaharwar AK, Rivera C, Wu C-J, Chan BK, Schmidt G. Photocrosslinked nanocomposite hydrogels from PEG and silica nanospheres: Structural, mechanical and cell adhesion characteristics. Materials Science and Engineering: C. 2013;33(3):1800–7.

APPENDIX

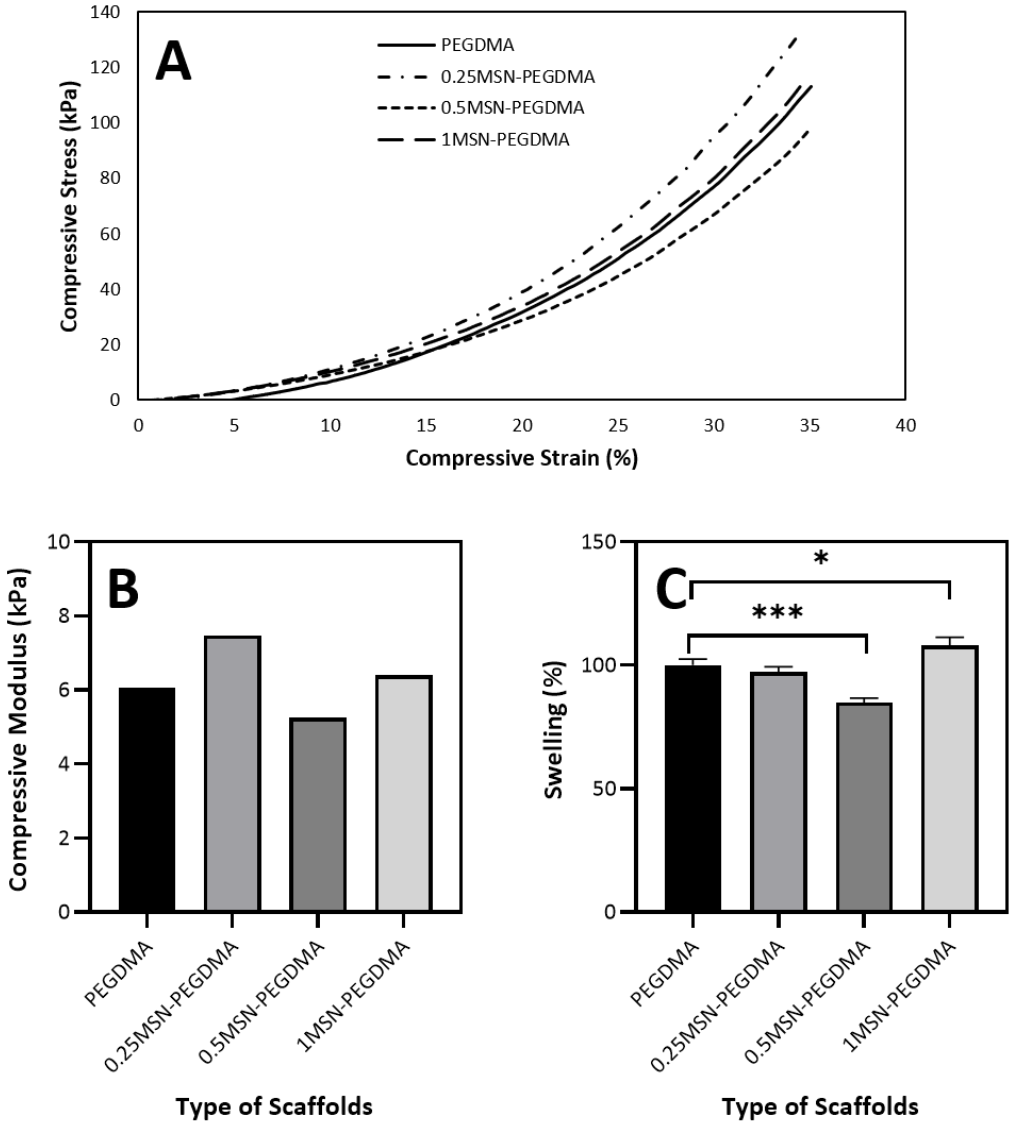

Appendix 1. A, B) Compression and **C)** swelling analysis data of PEGDMA scaffolds incorporated with MSNs at different ratios. Statistical analysis for swelling test was performed with ordinary one-way ANOVA followed by Dunnett's multiple comparison test with significance levels of p*<0.05 and p***<0.001.

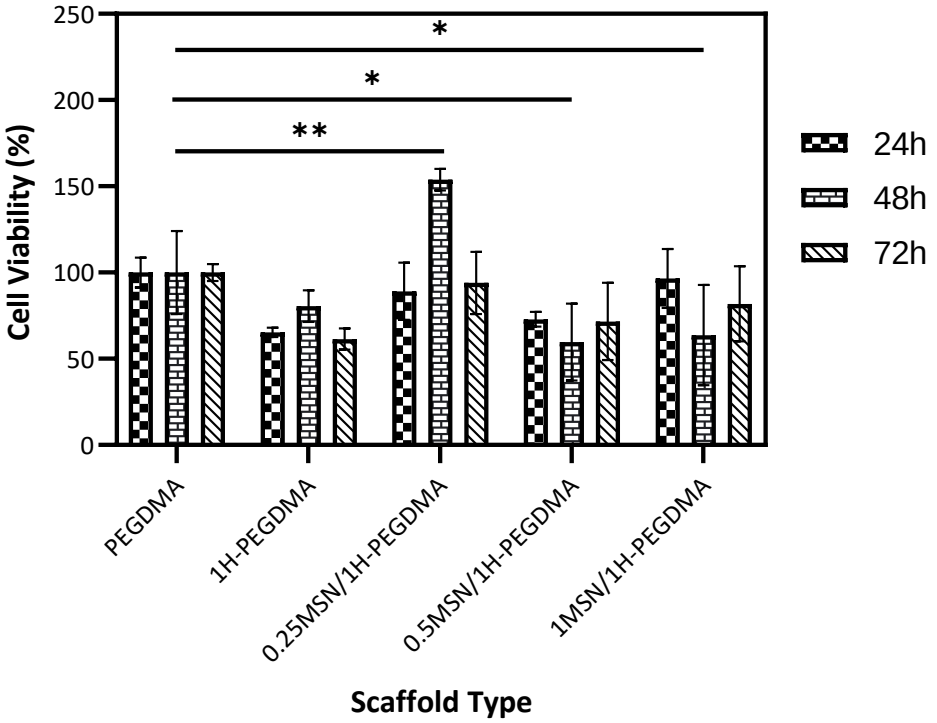

Appendix 2. Viability analysis of cell encapsulated PEGDMA, 0.25MSN/1H-PEGDMA, 0.5MSN/1H-PEGDMA, and 1MSN/1H-PEGDMA scaffolds. Statistical analysis was performed with ordinary two-way ANOVA followed by Dunnett's multiple comparison test with a significance level of $p^{*}<0.05$.

CURRICULUM VITAE

Personal Information:

Name-Surname: Ayşenur Pamukçu

E-mail: aysenurpamukcu@hotmail.com

Education:

- **2018-Ongoing, MSc in Biomedical Technologies**
  Izmir Katip Celebi University, Izmir, Turkey.
- **2014–2018, BSc in Bioengineering**
  Manisa Celal Bayar University, Manisa, Turkey.

List of Publications:

1. Eroglu, E., Portakal, H.S., **Pamukcu, A.** A New Generation Nanotherapeutic: pHEMA-Chitosan Nanocomposites in siRNA Delivery. 2020, Current Nanoscience, 16, 1-10.
2. **Pamukcu, A.,** Kaba, F., Sen Karaman, D. Tuning the Tensile Strength of Electrospun Fibers by Mesoporous Silica Nanoparticle Integration for Tissue Engineering Applications. 2019, IEEE Xplore.
3. **Pamukcu, A.,** Portakal, H.S., Eroglu, E. New Generation Biomaterials Used in Delivery of Therapeutic Molecules. 2018, Erzincan University Journal of Science and Technology, 11(3), 524-542.

Proceedings:

1. **Pamukcu, A.,** Kaba, F., Sen Karaman, D. Tuning the Tensile Strength of Electrospun Fibers by Mesoporous Silica Nanoparticle Integration for Tissue Engineering Applications. TIPTEKNO'19 Medical Technologies Congress, Izmir, October 2019.
2. Durna, G., Celebi, K., Bakay, E., **Pamukcu, A.,** Topaloglu Avsar, N., Sen Karaman, D. "Combinatory Antimictobial Photodynamic Threaphy with Silica Nanoparticles ", 4th GTU Photodynamic Day, Gebze, Kocaeli, April 2019.
3. Portakal, H.S., **Pamukcu, A.,** Eroglu, E. "A Novel Approach to Gene Therapy: Synthesis and Characterization of pHEMA-Chitosan Nanospheres Loaded with siRNA." 14th Nanoscience and Nanotechnology Conference, Izmir, 2018.
4. **Pamukcu, A.,** Portakal, H.S., Eroglu, E. "Synthesis and Characterization of pHEMA Chitosan Nanospheres Encapsulated with an Anticancer Agent, Resveratrol." I. International University Industry Cooperation, R&D and Innovation Congress, Manisa, 2017.